

RESEARCH

Open Access



# Microbial community dynamics in electroactive biofilms across time under different applied anode potentials

Chao-Chin Chang<sup>1</sup>, Yu-Chun Chen<sup>1</sup> and Chang-Ping Yu<sup>1,2\*</sup>

## Abstract

In bioelectrochemical wastewater treatment systems, electrochemically active bacteria (EAB) in the anode can simultaneously treat wastewater and produce electricity via extracellular electron transfer. The anode potential has been reported as one way for selecting EAB; though, conflicting results of the relationship between applied potentials and the performance and community composition of EAB have been reported. In this study, we investigated the cultivation time and applied anode potentials (+0.2, 0, -0.2, and -0.4 V vs. Ag/AgCl) on the performance of current production and the compositions of the microbial community. Our results showed that the applied potentials affected the performance of current production, but the effect was substantially reduced with cultivation time. Particularly, the current gradually increased from negative to positive values with time for the applied anode potential at -0.4 V, implying the anode biofilm shifted from accepting electrons to producing electrons. In addition, principal coordinates analysis results indicated that microbial community compositions became closer to each other after long-term enrichment. Subsequently, principal component analysis demonstrated that systems with applied potentials from +0.2, 0 to -0.2 V and at -0.4 V were, respectively, reclassified into principal component 1 (higher-energy-harvesting group) and principal component 2 (lower-energy-harvesting group), implying in addition to cultivation time, the amount of energy available for bacterial growth is another key factor that influences EAB populations. Overall, this study has demonstrated that the selected cultivation time and the particular anode potentials applied in the study determine whether the applied anode potentials would affect the community and performance of EAB.

**Keywords:** Poised anode potentials, Current production, Microbial community, Electrochemically active bacteria, Principal component analysis

## 1 Introduction

It has been observed that electrochemically active bacteria (EAB) are capable of simultaneously treating wastewater and producing environmentally friendly “green” electricity in the bioelectrochemical wastewater treatment system through direct and indirect extracellular electron transfer (EET) (Fig. S1 in Supplementary Material). The cultivation of EAB has attracted wide attention

[1, 2], and diverse EAB have been found [3]. Controlling poised anode potential is considered as one of the methods to cultivate different EAB [4], but contrasting viewpoints have also been suggested in previous studies. On one hand, when EAB were cultivated under certain poised anode potential, some studies reported biomass, power density [5, 6], and acceleration or suppression of EET rates in the microbial community [7] could be observed as a function of applied potential. To adapt the applied potential and harvest energy, EAB were found to be capable of changing the relative abundance of  $\text{NAD}^+$  and  $\text{NADH}$  to optimize the exploitation of the

\* Correspondence: [cpyu@ntu.edu.tw](mailto:cpyu@ntu.edu.tw)

<sup>1</sup>Graduate Institute of Environmental Engineering, National Taiwan University, Taipei 10617, Taiwan

<sup>2</sup>Water Innovation, Low Carbon and Environmental Sustainability Research Center, National Taiwan University, Taipei 10617, Taiwan



© The Author(s). 2022 **Open Access** This article is licensed under a Creative Commons Attribution 4.0 International License, which permits use, sharing, adaptation, distribution and reproduction in any medium or format, as long as you give appropriate credit to the original author(s) and the source, provide a link to the Creative Commons licence, and indicate if changes were made. The images or other third party material in this article are included in the article's Creative Commons licence, unless indicated otherwise in a credit line to the material. If material is not included in the article's Creative Commons licence and your intended use is not permitted by statutory regulation or exceeds the permitted use, you will need to obtain permission directly from the copyright holder. To view a copy of this licence, visit <http://creativecommons.org/licenses/by/4.0/>.

thermodynamic frame, and hence, competition among mixed cultures of microorganisms is unavoidable [8]. *Shewanella oneidensis* MR-1, as a model of EAB, has been further proposed to be capable of sensing and responding to electrodes by regulating catabolic pathways at the molecular level [9]. On the other hand, some studies considered activities of EAB would not be affected by applied anode potential [10].

To further investigate this controversial phenomenon, we preliminarily compared results reported in previous studies about the electrical performance of bioelectrochemical systems utilizing acetate as the substrate under different poised potentials. Inconsistent results were observed regarding the maximum current performance, which was respectively obtained at  $-0.4$ ,  $-0.3$ ,  $-0.2$  and  $0.4$  V vs. Ag/AgCl [4, 11–14], as shown in Table 1. A wide range of potentials to achieve the maximum current output has been observed in previous studies. Whether the applied potential could affect the activities of EAB and whether better applied potential could be identified in complex mixed cultured systems remain unclear. Therefore, more research is needed to reveal the key factors affecting the relationship among applied potentials, microbial communities and the performance of controlled bioelectrochemical systems.

In this study, we hypothesize that competition for harvesting energy among mixed cultures of microorganisms continuously exists, and the effect of applied potentials on the performance and microbial community composition may change with cultivation time. Cultivation time could be one of the important factors in shaping the relationship between applied potentials and controlled bioelectrochemical systems, but it was less discussed. Therefore, systems which had four different applied potentials were cultivated for over 3 months, and statistical comparisons of the performance and microbial community composition among them were conducted at three substages: substage 1 (1–34 d), substage 2 (35–50 d),

and substage 3 (51–67 d). Moreover, multivariate analysis techniques, such as principal component analysis (PCA), which can create one or more new index variables (i.e., principal components, PCs), can assist us in extracting useful features by re-exploring and re-classifying our data [15–17]. Hence, the relationship between poised potentials and microbial community compositions of controlled bioelectrochemical systems over long-term operation will be further revealed by PCA in this study.

## 2 Materials and methods

### 2.1 Reactor configuration and operation

In this study, we constructed two-chamber H-type microbial fuel cell (MFC) systems, which were composed of an anode chamber and a cathode chamber, separated by a proton exchange membrane (Nafion 117, DuPont, United States). The effective volume of these systems was 300 mL (anode 150 mL, cathode 150 mL), and the diameter of the proton exchange membrane was 3.2 cm.

Four MFC systems were operated with every anode chamber being inoculated with 50 mL of anaerobic sludge (Dihua wastewater treatment plant, Taipei, Taiwan), and the influent synthetic wastewater contained  $0.732$  g L<sup>-1</sup> sodium acetate (i.e., 570 mg L<sup>-1</sup> Chemical Oxygen Demand),  $0.1$  g L<sup>-1</sup> ammonium chloride,  $3$  g L<sup>-1</sup> potassium phosphate,  $6.065$  g L<sup>-1</sup> potassium dihydrogen,  $0.5$  g L<sup>-1</sup> sodium chloride, and other trace elements as growth nutrients, namely, MgSO<sub>4</sub>·7H<sub>2</sub>O, 100; CaCl<sub>2</sub>·2H<sub>2</sub>O, 15; MnSO<sub>4</sub>·H<sub>2</sub>O, 3.4; FeCl<sub>2</sub>·4H<sub>2</sub>O, 2; (NH<sub>4</sub>)<sub>6</sub>Mo<sub>7</sub>O<sub>24</sub>·4H<sub>2</sub>O, 1.2; CuSO<sub>4</sub>·5H<sub>2</sub>O, 1.26; and Zn(NO<sub>3</sub>)<sub>2</sub>·6H<sub>2</sub>O, 1.8 (in mg L<sup>-1</sup>). In each cathode chamber, 50 mM potassium ferricyanide buffer solution (containing 16.462 g L<sup>-1</sup> potassium ferricyanide, 25.461 g L<sup>-1</sup> potassium phosphate, and 3.535 g L<sup>-1</sup> potassium dihydrogen) was used as the electron acceptor. The two-chamber H-type MFC systems were operated under batch mode with a hydraulic retention time of 2 d.

**Table 1** Comparisons of acetate-based systems utilizing applied potential to harvest anode EAB

Inoculum	Applied potential (V vs Ag/AgCl)	Cultivation time	Potential achieved maximum current (V)	Substrate	Reference
Effluent of acetate-fed MFCs	$-0.4, -0.2, 0$	33 d (792 h)	$-0.2$	Acetate	[4]
<i>Geobacter sulfurreducens</i>	$+0.2, +0.3, +0.4, +0.5, +0.6, +0.7, +0.8$	~ 4 d (98 h)	$+0.4$	Acetate	[11]
Activated sludge	$-0.42, -0.36, -0.25, +0.1$	30 d (720 h)	$-0.42$	Acetate	[12]
<i>Geobacter soli</i>	$-0.4, -0.2, 0, +0.2, +0.4, +0.6$	~ 4 d (~96 h)	$-0.2$	Acetate	[13]
Effluent of acetate-fed MECs	$-0.45, -0.29, +0.01, +0.31, +0.61$	25 d (600 h)	$-0.29$	Acetate	[14]
Anaerobic sludge	$-0.4, -0.2, 0, +0.2$	67 d (1608 h)	0	Acetate	this study

Carbon felt was used as the electrode with an area of 25 cm<sup>2</sup> (5 × 5 cm) in both the anode and cathode chambers. These four chambers were connected with a multi-potentiostat (PalmSens4C, Palmsens BV, Netherlands) at poised anode potentials of +0.2, 0, -0.2, and -0.4 V (vs. Ag/AgCl) (denoted as anode\_+0.2V, anode\_0V, anode\_-0.2V, anode\_-0.4V) throughout the entirety of the experiment.

The operation period can be divided into three sub-stages, as shown in Fig. 1. Anodic biofilms cultivated at four poised potentials were sampled three times, i.e., on day 34 (substage 1: 1–34 d), day 50 (substage 2: 35–50 d), and day 67 (substage 3: 51–67 d). After substage 3, the electrochemical and morphological properties of biofilms cultivated at four poised potentials were analyzed by cyclic voltammetry (CV) and scanning electron microscopy (SEM).

## 2.2 Measurement of current production and electrochemical properties

During the operation, systems were constructed with anodic carbon felt as the working electrode, cathodic carbon felt as the counter electrode, and a reference electrode (Ag/AgCl) being inserted into the anode chamber. After substage 3, the electrochemical properties of the anodic biofilms were tested by CV (working electrode: anodic carbon felt; counter electrode: platinum electrode in the anode; reference electrode: Ag/AgCl electrode in the anode) using a potentiostat (SP-150, Bio-Logic Science Instruments, France) with a potential range from -0.6 to +0.4 V (vs. Ag/AgCl) and a scan rate of 10 mV s<sup>-1</sup>. In addition, in order to statistically compare the current production among the four systems at different substages, p-values were calculated by using analysis of variance tests according to a previous literature [18].

## 2.3 Microbial community and morphology analyses

To identify the microbial community, the original sludge and anodic biofilm were sampled from substage 1 to 3. During sampling, the electrode samples were cut into smaller pieces that contained both the electrode and biofilms. DNA was extracted from the original sludge and the anodic biofilm samples using a DNeasy PowerSoil Kit (Cat No./ID: 12888-100, QIAGEN, Germany) in accordance with the manufacturers' instruction. The DNA concentrations of all samples were quantified using a nanodrop microvolume spectrophotometer (NanoDrop 1000 Spectrophotometer V3.8, Thermo Fisher Scientific, United States). The polymerase chain reaction primers were utilized for the hypervariable V3 and V4 regions of bacterial 16S rRNA gene high throughput sequencing with a set of 341F (5'-CCTACGGGNGGCWGCAG-3') and 805R (5'-GACTACHVGGGTATCTAATCC-3').

After each sample was tagged with dual indexes, the total initial reads were processed to obtain the effective reads. These effective reads were subsequently sent to Mothur v.1.33.3 and QIIME v1.80 (containing the Greengenes 16S rRNA Taxonomy Database) to analyze 16S rRNA gene sequences of the microbial communities of biofilms. After the operational taxonomic unit (OTU) was clustered with a cutoff of 97% identity using an average neighbor algorithm [19], the non-redundant sequence number was used as the eventual usable OTU number. In addition, all anode samples for SEM were fixed in a 2.5% solution of paraformaldehyde and processed through an ethanol dehydration series (i.e., 30%, 50%, 70%, 90%, 100% v/v EtOH, 20 min for each treatment), and then dried to preserve the structure of the bacteria in the freeze dry system (Cole-Parmer, Labconco). After that, all samples were coated with platinum by an ion sputter coater, and observed using SEM (TM-3000, HITACHI, Japan).

## 2.4 Statistical analyses of the microbial community composition

In this study, to quantify the alpha and beta diversities among microbial community of biofilms under different applied potentials, the Shannon diversity index was used to characterize species diversity and account for the abundance and evenness of the species [20, 21]. In addition, comparisons of microbial communities among the four applied potentials at different substages were statistically investigated using principal coordinates analysis (PCoA) [22] and Bray-Curtis similarity [23].

In addition to using the Shannon diversity index and PCoA to evaluate the complicated relationship between controlled bioelectrochemical systems and different applied potentials during the three substages, reducing the number of variables can also provide us with simplified but comprehensive information. Hence, we utilized the multivariate analysis PCA to produce a smaller number of new variables (i.e., PCs) that contain sufficient information on the original dataset [16]. PCA, which is a type of multivariate analysis, was developed by [24]. By utilizing this method, we can construct a table that summarizes intercorrelated quantitative dependent variables. Thus, we can extract useful and essential information from it [15]. In this study, Kaiser-Meyer-Olkin (KMO) and Bartlett tests were tested first, and it can be passed unless KMO is higher than 0.6, and the significance was lower than 0.01. Regarding the chosen of PCs can be decided by Scree plots. Because the variance of each standardized variable is 1, if the factor's capability of explaining the variability is smaller than 1, this means that the efficacy is worse than one variable, and hence, eigenvalues higher than 1 were chosen and defined as PCs [15]. Rotated component matrix were comprehensively investigated throughout all

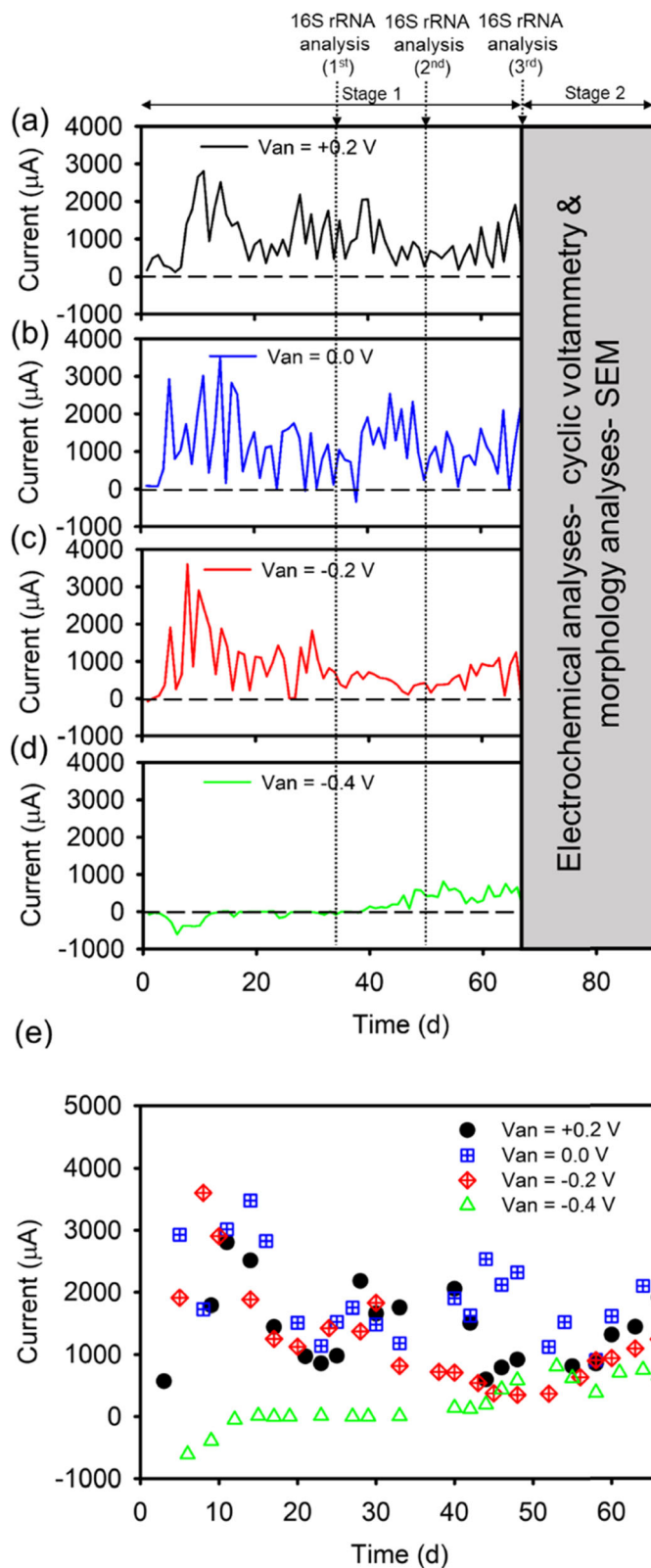


**Fig. 1** Current production at four poised potentials from substage 1 to 3 and electrochemical and morphology analyses after substage 3. (a) anode cultivated at poised potential of +0.2 V; (b) anode cultivated at poised potential of 0 V; (c) anode cultivated at poised potential of -0.2 V; (d) anode cultivated at poised potential of -0.4 V; (e) peak current production at four poised potentials from substage 1 to 3

PCAs. Loadings higher than 0.75 in PCs, representing those variables that were important contributors to each given PC, were chosen in this study [25].

### 3 Results

#### 3.1 Current production and electrochemical analyses

The operation period was divided into three substages, as shown in Fig. 1. During the operation (1–67 d), anodes were connected with a multi-potentiostat at a poised anode potential of +0.2, 0, –0.2, and –0.4 V (vs. Ag/AgCl) throughout the entire experiment. Their respective performances observed during the long-term operation demonstrated distinct properties as shown in Table 2. For the anode cultivated at +0.2 V (denoted as anode\_+0.2V), the average output current reached its peak after about 1 month (substage 1) and then slowly decreased to about 949  $\mu\text{A}$  at substage 2. At substage 3, the average current output only reached 779  $\mu\text{A}$ . For the anode cultivated at 0 V (denoted as anode\_0V), it showed a relatively stable average current output greater than 1000  $\mu\text{A}$ . The highest current output was obtained at substage 2. For the anode cultivated at –0.2 V (denoted as anode\_–0.2V), although it peaked in the first month, it dropped sharply to 458  $\mu\text{A}$  during substage 2 and rose slightly to 600  $\mu\text{A}$  during substage 3. As for the anode cultivated at –0.4 V (denoted as anode\_–0.4V), the enrichment time was much longer than that of the other three, but the current output performed steadily and continuously increased from –105 to 475  $\mu\text{A}$ , implying the anode biofilm shifted from accepting electrons to producing electrons.

With regard to the electrochemical properties, CV (Fig. S2) was shown capable of describing anodic electron transfer [26], and hence, it was used for analyzing anodes before inoculation (i.e., containing only the electrode and substrate) and anodes after cultivation (tested after substage 3, containing the electrode, substrate, and biofilm) to evaluate the electrochemical activities of EAB. The results showed one pair of redox peaks in blank samples with an oxidation peak at 0.28 V and a reduction peak at 0.23 V, and hence, a midpoint potential was found at 0.25 V. After long-term cultivation, the current flow among the four scenarios was higher than

that for the blank one. For systems with higher applied potentials, i.e., anode\_+0.2V and anode\_0V, similar properties were found with no redox peak, but the high turnover current was observed, showing potential ranges of 0.1 to 0.4 V and –0.4 to +0.4 V (vs. Ag/AgCl), respectively. On the other hand, systems with lower potentials applied (anode\_–0.2V and anode\_–0.4V) collectively demonstrated redox peaks. For anode\_–0.2V, an oxidation peak was observed at –0.21 V, whereas the reduction peak was observed to be at the potential of –0.23 V, and hence, a midpoint potential was found at –0.22 V. For anode\_–0.4V, an oxidation peak was observed at –0.30 V, whereas the reduction peak was observed to be at the potential of –0.32 V, and hence, a midpoint potential was found at –0.31 V.

#### 3.2 Microbial community composition and morphology analyses of biofilms

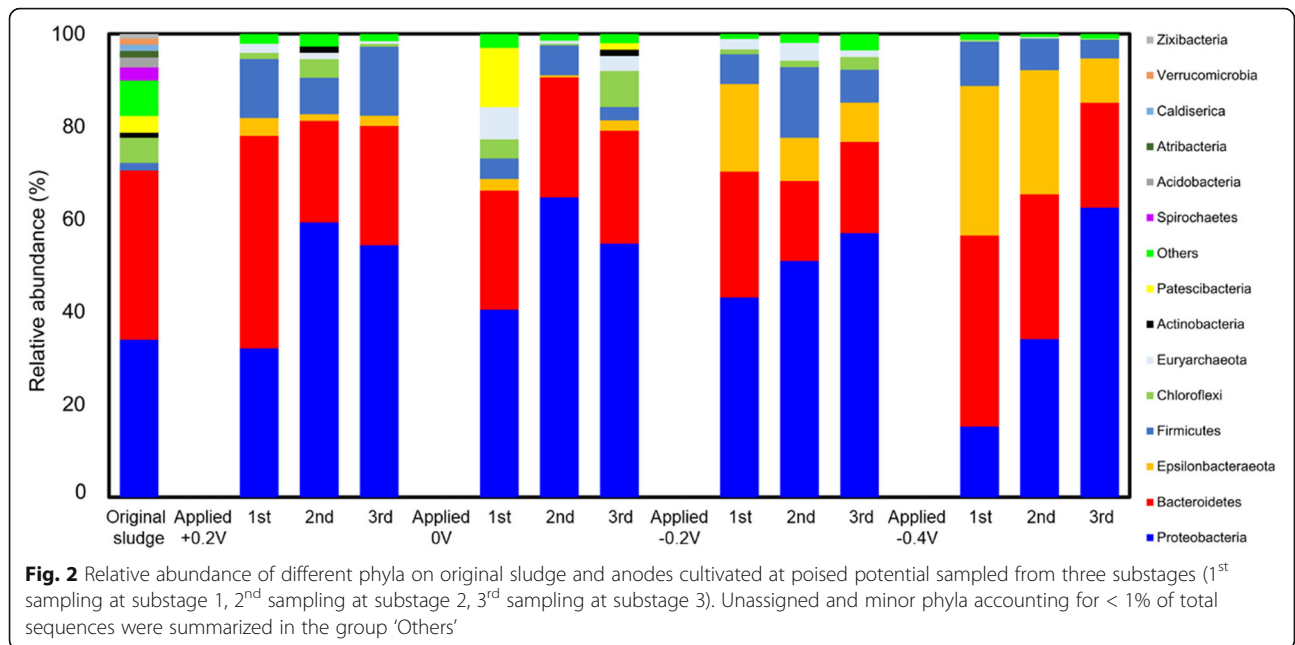
To further investigate the impact of cultivation time on the microbial community composition at different poised potentials, the relative abundances of different phyla within the original sludge and anodes cultivated at different poised potential and sampled from the three substages are depicted in Fig. 2. In the original sludge, both *Bacteroidetes* and *Proteobacteria* were most dominant phyla and collectively accounted for more than 70%. After applying potentials on anodes, *Proteobacteria* in anode\_0V and anode\_–0.2V increased but dramatically decreased in anode\_–0.4V at substage 1. However, at substage 2, changes of *Proteobacteria* of four systems were similar, showing rising trend after over one-month cultivation. At substage 3, *Proteobacteria* of anode\_+0.2V and anode\_0V slowly decreased but increased in anode\_–0.2V and anode\_–0.4V.

Regarding the change of the predominant genera over cultivation time (Fig. 3), anode\_+0.2V showed a distinct difference between substages 1 and 3 and was observed to have 19.9% *Flavobacterium*, 9.9% *Pandora*, and 31.9% *Geobacter* in substages 1, 2 and 3, respectively. For anode\_0V, *Geobacter* had the highest percentages of 14.2% and 16.4% during substages 1 and 3, respectively, but during substage 2, *Acinetobacter* (42.0%) achieved the highest portion instead. For anode\_–0.2V, *Bacteroides* (21.1%)

**Table 2** Profiles of average current production at four poised potentials

Items	Stage	Time (d)	Current ( $\mu\text{A}$ ) output at +0.2 V	Current ( $\mu\text{A}$ ) output at 0 V	Current ( $\mu\text{A}$ ) output at –0.2 V	Current ( $\mu\text{A}$ ) output at –0.4 V	P value among four poised potentials
Current ( $\mu\text{A}$ )	Substage 1	1-34	1093 (744)*	1156 (967)	1130 (850)	–105 (155)	1.27E-11 (F value = 22.0)
	Substage 2	35-50	949 (559)	1240 (755)	458 (176)	186 (206)	1.97E-07 (F value = 15.1)
	Substage 3	51-67	779 (477)	1002 (612)	600 (381)	475 (195)	0.02 (F value = 3.5)

\*values in parentheses indicate standard deviation



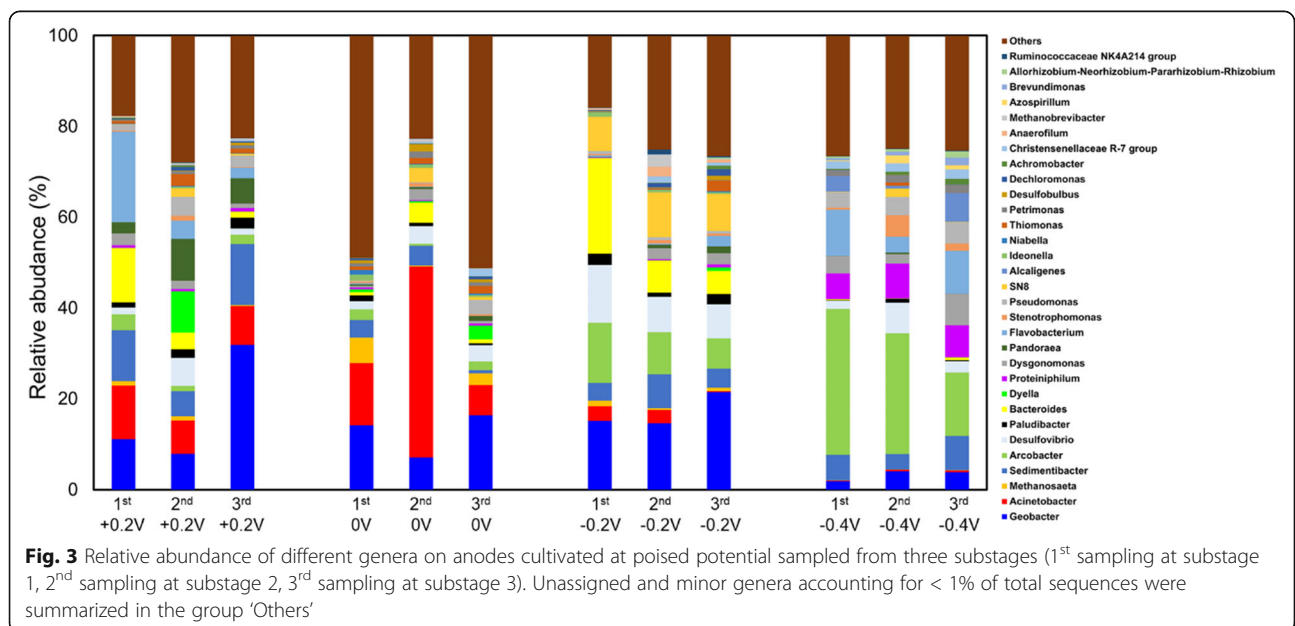
was the highest only during substage 1, but during substages 2 and 3, *Geobacter* continuously had the highest percentages of 14.6% and 21.5%, respectively. For anode<sub>-0.4V</sub>, *Arcobacter* continuously had the highest percentages of 32.1%, 26.6%, and 14.0% throughout all the three substages. Overall, all the above mentioned predominant genera belonged to only two phyla (i.e., *Proteobacteria* and *Bacteroidetes*).

Microbial morphology analyses of anode biofilms were conducted using SEM during after substage 3, as shown in Fig. S3. The SEM micrographs showed that the

bacteria were aggregated into biofilms and embedded in extracellular polymeric substances, but anode<sub>+0.2V</sub> was observed to be visually thicker than the other three anodes, which supports the theory that lower applied anode potentials enrich thinner biofilms, as reported in previous studies [6, 27, 28].

### 3.3 Microbial diversity analyses

In addition to the relative abundances of the microbial communities, in order to further quantify the microbial diversity within the samples, the Shannon diversity



indexes were calculated for the systems under the four poised potentials, as shown in Table 3. For anode<sub>+</sub>0.2V, the Shannon index during substage 1 was 4.86, then rose to 6.01 during substage 2, and fell sharply during substage 3. For anode<sub>0</sub>V, the Shannon index was at 6.00 during substage 1, dropped during substage 2, and rose to 6.29 during substage 3. For anode<sub>-</sub>0.2V, the index was 4.59 during substage 1, increased during substage 2 and further rose to 5.70 during substage 3. For anode<sub>-</sub>0.4V, a Shannon index of 4.26 was observed during substage 1, gradually increased during stage 2, and eventually reached 5.33 during substage 3. The results of Shannon index calculations indicate that when the applied potential was higher (anode<sub>+</sub>0.2V and anode<sub>0</sub>V), the biodiversity index fluctuated. On the other hand, when the potential was lower (anode<sub>-</sub>0.2V and anode<sub>-</sub>0.4V), the trend was distinct, and the biodiversity index rose gradually. In addition, across the four poised potentials, anode<sub>0</sub>V showed the highest Shannon index during substages 1 and 3, but during substage 2, anode<sub>+</sub>0.2V demonstrated the highest index.

In addition, comparisons of microbial communities under different anode potentials at respective substages were investigated by PCoA at the genus levels in Fig. 4 to further cluster the microbial communities of different samples. Results demonstrated that distances among all anode samples gradually reduced with cultivation time (especially for anode<sub>-</sub>0.2V and anode<sub>-</sub>0.4V). Results from Bray-Curtis similarity indicated after long-term enrichment, the differences among microbial community under four anode potentials became smaller (increasing Median value) within substages. Both results indicated that the microbial community compositions under the four poised potentials changed and became closer to each other with longer enrichment time.

**3.4 Multivariate analysis: PCA**

Multivariate statistical methods, such as PCA, can be useful in reducing the number of 12 original variables and creating one or more new index variables (i.e., PCs) with sufficient information from the original dataset to illustrate the relationship between variables and microbial compositions of EAB. During the process of PCA, KMO and Bartlett assessment were tested first, and the results indicated that KMO is 0.79, which is higher than

**Table 3** Shannon’s diversity index at four poised potentials

Poised potential (mV)	Substage 1	Substage 2	Substage 3
+200	4.86	6.01	4.51
0	6.00	4.05	6.29
-200	4.59	5.45	5.70
-400	4.26	4.90	5.33

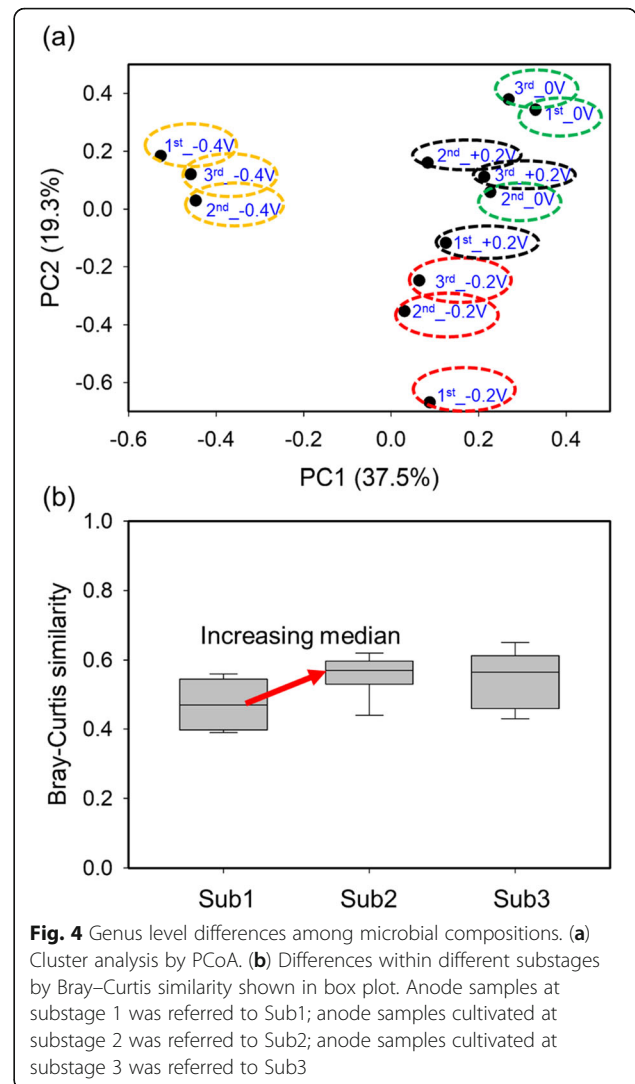


**Fig. 4** Genus level differences among microbial compositions. (a) Cluster analysis by PCoA. (b) Differences within different substages by Bray-Curtis similarity shown in box plot. Anode samples at substage 1 was referred to Sub1; anode samples cultivated at substage 2 was referred to Sub2; anode samples cultivated at substage 3 was referred to Sub3

0.60, and the significance was also lower than 0.01, indicating that this case is suitable for PCA.

With regard to the chosen meaningful PCs, a Scree plot, as shown in Fig. 5a, was made. Two PCs (denoted as PC1 and PC2) were found in our case. In addition, we further checked the explained variance of PCs (Table 4). For PC1, up to 66.4% variance can be explained, and for PC2, 12.4% can be explained. Two components can collectively explain 78.8%, which means that instead of the original 12 variables, by utilizing only two reconstructed PCs, we can describe the original situation. Furthermore, a rotated component matrix for PC1 and PC2 with 12 loadings in each PC is drawn and shown in Fig. 5b. The 12 loadings represent the correlation between the PC and the 12 original variables, with a constrained range between -1 and +1, and higher loadings represent those variables that are important contributors to each given PC. PC1 simultaneously contained samples with applied potentials ranging from +0.2 to -0.2 V through the three

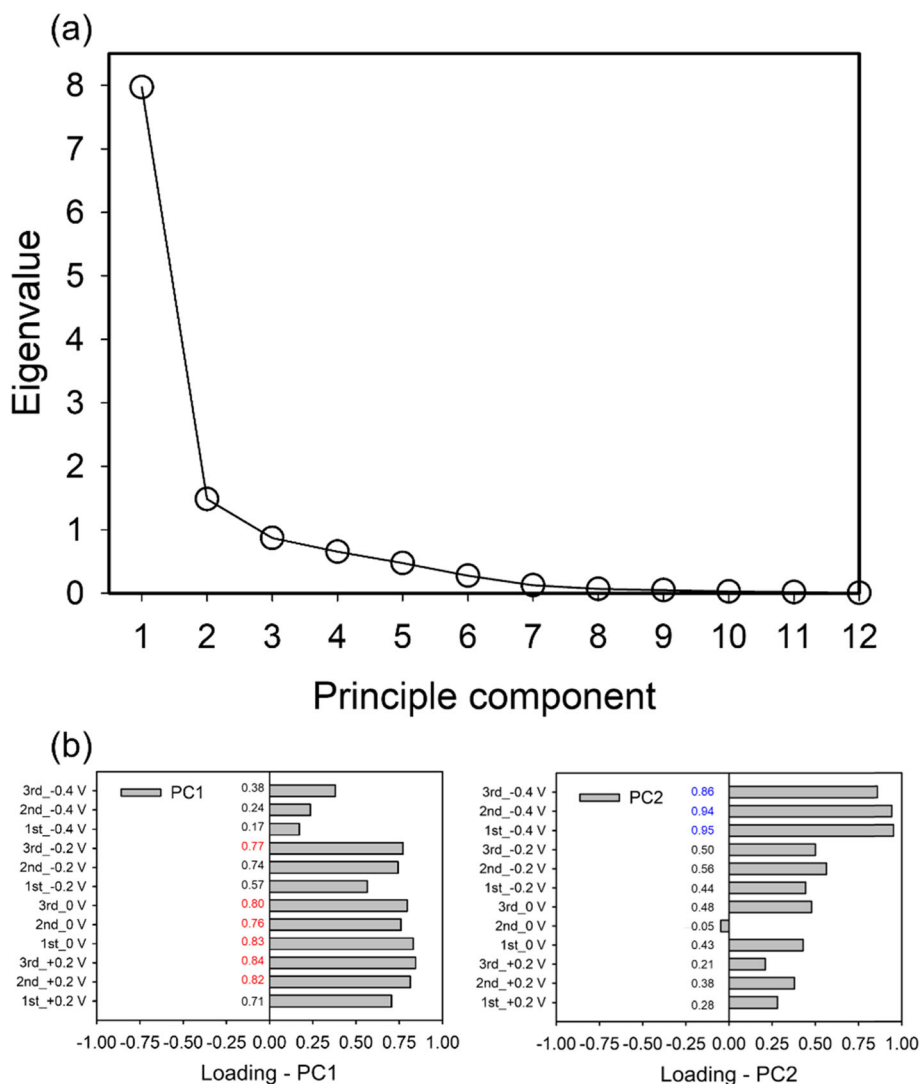


**Fig. 5** Scree plots and Rotated component matrix of PC1 and PC2 in PCA analysis. (a) Scree plot. (b) Rotated component matrix of PC1 and PC2 and marked variables (red in PC1, blue in PC2) when loadings were higher than 0.75

substages. PC2 simultaneously contained samples with an applied potential at -0.4 V through the three substages, and hence, we suggest that PC1 can be renamed as a high-energy-harvesting group and PC2 as a low-energy-harvesting group. There might be a key potential threshold between the groups, which seemed to be between -0.2 and -0.4 V. Poisoning anode potentials above or below this threshold will select microbial community compositions with largely different energy harvesting abilities.

#### 4 Discussion

Fluctuating current production was observed collectively for anodes cultivated at four applied potentials, and performance comparisons among the four scenarios changed with time as shown in the Fig. 1. During substage 1,

anode\_0V was better than anode\_-0.2V, anode\_-0.2V was better than anode\_+0.2V, and anode\_+0.2V was better than anode\_-0.4V. During substage 2, anode\_0V was better than anode\_+0.2V, anode\_+0.2V was better than anode\_-0.2V, and anode\_-0.2V was better than anode\_-0.4V. During substage 3, the same relationship was observed as that in substage 2, and anode\_0V and anode\_-0.4V showed better and worse performance, respectively. The p-values (i.e., significantly different when the p-value is < 0.01) were calculated to statistically compare current production among the four systems at the different substages [18] and are summarized in Table 2. The results show that at substages 1, the differences among the four systems (anodes connected with a multipotentiostat at a poised anode potential of +0.2, 0, -0.2, and -0.4 V vs. Ag/AgCl) were determined to be

**Table 4** Explained variances among all samples in PCA analysis

Component	Eigenvalue	Variance (%)	Accumulated variance (%)
PC 1	7.968	66.40	66.40
PC 2	1.484	12.37	78.77
PC 3	0.869	7.24	86.01
PC 4	0.653	5.44	91.45
PC 5	0.474	3.95	95.40
PC 6	0.274	2.28	97.68
PC 7	0.123	1.02	98.70
PC 8	0.065	0.54	99.24
PC 9	0.046	0.38	99.62
PC 10	0.025	0.21	99.83
PC 11	0.016	0.14	99.96
PC 12	0.004	0.04	100.00

statistically significant, and the differences among them decreased at substage 2. Furthermore, at substage 3, differences among them showed no statistically significant difference with the p-value dramatically increasing. The effect of cultivation time could also illustrate why a wide range of poised potentials has been observed to achieve maximum current output in previous studies [4, 11–14].

To further identify which poised voltage system contributed to the increasing p value, follow-up pairwise significance tests among three substages were conducted and listed in Tables S1 and S2. Results indicated during substage 1, the significant difference was largely contributed by the anode<sub>-0.4V</sub>. During substage 2, the significant difference was also mainly contributed by the anode<sub>-0.4V</sub>, but the p value increased, suggesting the difference between anode<sub>-0.4V</sub> and other systems decreased. During substage 3, no significant difference was observed among different systems. The increase of the p-value among the four applied potentials after long-term cultivation suggested that the effect of the applied anode potentials on the performance of the EAB substantially reduced with cultivation time. In addition, the follow-up pairwise significance tests among three substages further illustrated the reducing effect may be mainly contributed by the decreasing difference between anode<sub>-0.4V</sub> and other systems.

With regard to the electrochemical properties, the difference between higher and lower applied potentials indicate that different EAB can evolve to adapt to the electrodes poised at different potentials, as in the previous study [12]. In addition, from a thermodynamic perspective, acetate, which has a standard biological potential of  $-0.496$  V vs. Ag/AgCl [29, 30], was used as a substrate in this study. Therefore, the energy difference between  $-0.496$  V (i.e., the electron donor) and  $+0.2$ ,  $0$ ,  $-0.2$ , and  $-0.4$  V of the poised anode potentials (i.e., the

terminal electron acceptors) contributed to the maximum thermodynamic frame in this study. When the poised potentials were  $+0.2$ ,  $0$ ,  $-0.2$ , and  $-0.4$  V, current was generated at about  $0.1$ ,  $-0.4$ ,  $-0.2$ , and  $-0.3$  V, respectively, as described by CV (Fig. S2). The very low onset potential of anode<sub>0V</sub> indicating EAB in this system can harvest the least amount of energy to maintain cell growth ( $-0.496$  to  $-0.4$  V) but produces the highest current ( $-0.4$  to  $0.1$  V). This, on the other hand, provides some evidence to illustrate why anode<sub>0V</sub> performed better during the three substages continuously, as described by the current production (Fig. 1).

With regard to the microbial community composition, *Geobacter*, an important exoelectrogen [31–33], was found to be enriched at anode by different applied anode potentials [11, 13, 34]. *Geobacter* was respectively observed to account for the highest percentage at the applied potentials of  $-0.2$  V [12] or  $+0.2$  V [6, 35], and these conflicting results were also observed in this study. During substage 1 and substage 2, the anode<sub>-0.2V</sub> system was observed to have the highest percentage of *Geobacter* of 15.1 and 14.6%. Nevertheless, during substage 3, anode<sub>+0.2V</sub> was observed to have the highest percentage of *Geobacter* of 31.9% among the four poised potentials. In addition to *Geobacter*, *Acinetobacter* as one of EAB, was not only reported to be found abundantly in the cathodic biofilm [36, 37], capable of improving cathodic performance [38] but also observed in the anodic biofilm [39, 40]. Results indicated that *Acinetobacter* had higher percentage at anode<sub>+0.2V</sub> and anode<sub>0V</sub> (especially anode<sub>0V</sub> at substage 2), but showed very low percentage at anode<sub>-0.2V</sub> and anode<sub>-0.4V</sub> (all < 1% at anode<sub>-0.4V</sub> across three substages).

Electroactive microorganisms can transfer electrons to insoluble terminal electron acceptors, such as electrodes via EET. Different EET pathways (direct EET, cytochromes or nanowires; indirect EET, metabolites or redox mediators) as shown in the Fig. S1 contribute to the current production. Two different electroactive microorganisms, *Acinetobacter* and *Geobacter*, were observed as mentioned above. It is reported that the *Acinetobacter calcoaceticus* strain can demonstrate the indirect EET, utilizing self-excreted redox compound (pyrroloquinoline quinone) [41]. With regard to *Geobacter*, both direct EET pathways were found. Type IV pili (i.e. nanowire) can directly transport electrons from the inner membrane to an external electron acceptor. In addition, cytochromes on the outer membrane (especially c-type cytochrome Z) also contribute to the outer-membrane EET [42]. Overall, our results indicated in the mix-culture system, various electroactive microorganisms could collectively grow on the electrodes and demonstrate different EET pathways simultaneously.

On the other hand, *Arcobacter* was also reported to be one of EAB [43, 44], and found at biocathode [36], and it has been recently reported to be capable of accepting cathodic electrons under the redox potentials of  $-750$  mV (vs. Ag/AgCl) [45]. High percentage of this genus was found at anode $_{-0.2V}$  and anode $_{-0.4V}$  (especially anode $_{-0.4V}$  at substage 1). Higher potential electro-trophic bacteria (*Arcobacter*) but low electrogenic bacteria (*Geobacter*) may provide some information to illustrate why negative current production (i.e. electron uptake from electrode by microorganisms) was observed at anode $_{-0.4V}$  during substage 1 as shown in Table 2 and Fig. 1. Therefore, electron uptake from the electrode by electro-trophic bacteria and electron production from electrogenic bacteria to the electrode may collectively contribute to the current production and hence fluctuating phenomenon was observed.

Results from PCoA and Bray-Curtis similarity both indicated that the microbial community compositions under the four poised potentials changed and became closer to each other with longer enrichment time. Therefore, combined with the changes of electrical performance observed in Section 3.1 and the changes of the microbial community composition through the three substages found in this section, the fact that a potential has an effect on both performance and microbial communities was obviously observed, but the effect was gradually diminished with cultivation time. These results may provide the new viewpoint to illustrate why controversial results were obtained regarding effects of applied potential on the microbial community composition and why inconsistent results of EAB performance were observed. Cultivation time should be one of the important factors in changing the relationship between applied anode potentials and EAB.

In addition, PC1 as a high-energy-harvesting group (+0.2V to  $-0.2V$ ) and PC2 as a low-energy-harvesting group ( $-0.4V$ ) were found in this case, which indicated when poisoning anode potentials above this threshold, i.e.  $-0.2$  V, 0 V and +0.2 V in this study, more similar microbial community compositions could be grown on anodes. Therefore, in addition to cultivation time being observed to affect the microbial community composition under poised anode potential using PCoA, results of PCA indicated that choosing the applied potential range will be another key factor in determining the microbial community composition. The PCA results provide another new viewpoint to illustrate why it was controversial to consider whether the applied potential would affect the microbial community composition [1, 4, 10, 11].

## 5 Conclusions

This study investigated the relationship between applied anode potentials and the performance and community

of EAB. We observed that the effect of the applied potentials on the performance of the EAB substantially reduced with cultivation time. For the anode $_{-0.4V}$ , the current gradually shifted from negative to positive values with time, suggesting the anode biofilm shifted from accepting electrons to producing electrons. The PCoA results showed that the microbial community compositions among the four applied potentials became more similar with cultivation time, especially for anode $_{-0.2V}$  and anode $_{-0.4V}$ . PCA results reclassified microbial community samples into PC1 (higher-energy-harvesting group, from +0.2 to  $-0.2$  V) and PC2 (lower-energy-harvesting group, at  $-0.4$  V), indicating the amount of energy that can be harvested by microorganisms is vital, and the particularly low anode potential will select the unique EAB community utilizing limited energy for growth. Overall, our findings have demonstrated that the cultivation time and the applied anode potentials together affect the community and performance of EAB.

## 6 Supplementary Information

The online version contains supplementary material available at <https://doi.org/10.1186/s42834-022-00128-9>.

**Additional file 1: Table S1.** Original current profiles of follow-up pairwise significance tests among three substages. **Table S2.** Peak current profiles of follow-up pairwise significance tests among three substages. **Fig. S1.** Schematic diagram of extracellular electron transfer pathways [1]. **Fig. S2.** Comparisons between blank (black line) and anode cultivated at poised potential measured by cyclic voltammetry after substage 3. **(a)** anode cultivated at poised potential of +0.2 V; **(b)** anode cultivated at poised potential of 0 V; **(c)** anode cultivated at poised potential of  $-0.2$  V; **(d)** anode cultivated at poised potential of  $-0.4$  V. **Fig. S3.** Morphology analyses by SEM after substage 3. **(a)** anode cultivated at poised potential of +0.2 V; **(b)** anode cultivated at poised potential of 0 V; **(c)** anode cultivated at poised potential of  $-0.2$  V; **(d)** anode cultivated at poised potential of  $-0.4$  V.

### Acknowledgements

The authors gratefully acknowledge the financial support from the Ministry of Science and Technology, Taiwan, R.O.C., under grants MOST 108-2221-E-002-118-MY2 and 109-2221-E-002-084-MY2, and from National Taiwan University under the Excellence Improvement Program for Doctoral Students.

### Authors' contributions

CY and YC conceived and designed research. YC conducted experiments. CC contributed new analytical tools. CC and YC analyzed data. CC and CY wrote the manuscript. All authors read and approved the manuscript.

### Funding

This research was supported by the Ministry of Science and Technology, Taiwan, R.O.C., under grants MOST 108-2221-E-002-118-MY2 and 109-2221-E-002-084-MY2. This article was also subsidized by National Taiwan University under the Excellence Improvement Program for Doctoral Students.

### Availability of data and materials

The datasets generated during and/or analyzed during the current study are available from the corresponding author on reasonable request.

### Declarations

### Competing interests

All authors declare that they have no competing interest.

Received: 7 September 2021 Accepted: 22 February 2022

Published online: 21 March 2022

## References

- Koch C, Harnisch F. Is there a specific ecological niche for electroactive microorganisms? *ChemElectroChem* 2016;3:1282–95.
- Sydow A, Krieg T, Mayer F, Schrader J, Holtmann D. Electroactive bacteria—molecular mechanisms and genetic tools. *Appl Microbiol Biot*. 2014;98:8481–95.
- Feng CJ, Sharma SCD, Yu CP. Microbial fuel cells for wastewater treatment. In: Pacheco Torgal F, Labrincha JA, Diamanti MV, Yu CP, Lee HK, editors. *Biotechnologies and biomimetics for civil engineering*. Cham: Springer; 2015. p. 411–37.
- Aelterman P, Freguia S, Keller J, Verstraete W, Rabaey K. The anode potential regulates bacterial activity in microbial fuel cells. *Appl Microbiol Biot*. 2008;78:409–18.
- Carmona-Martinez AA, Harnisch F, Kuhlicke U, Neu TR, Schroder U. Electron transfer and biofilm formation of *Shewanella putrefaciens* as function of anode potential. *Bioelectrochemistry*. 2013;93:23–9.
- Wei JC, Liang P, Cao XX, Huang X. A new insight into potential regulation on growth and power generation of *Geobacter sulfurreducens* in microbial fuel cells based on energy viewpoint. *Environ Sci Technol*. 2010;44:3187–91.
- Ishii S, Suzuki S, Norden-Krichmar TM, Phan T, Wanger G, Nealon KH, et al. Microbial population and functional dynamics associated with surface potential and carbon metabolism. *ISME J*. 2014;8:963–78.
- Korth B, Harnisch F. Spotlight on the energy harvest of electroactive microorganisms: the impact of the applied anode potential. *Front Microbiol*. 2019;10:01352.
- Hirose A, Kasai T, Aoki M, Umemura T, Watanabe K, Kouzuma A. Electrochemically active bacteria sense electrode potentials for regulating catabolic pathways. *Nat Commun*. 2018;9:1083.
- Zhu XP, Yates MD, Hatzell MC, Rao HA, Saikaly PE, Logan BE. Microbial community composition is unaffected by anode potential. *Environ Sci Technol*. 2014;48:1352–8.
- Li DB, Li J, Liu DF, Ma X, Cheng L, Li WW, et al. Potential regulates metabolism and extracellular respiration of electroactive *Geobacter* biofilm. *Biotechnol Bioeng*. 2019;116:961–71.
- Torres CI, Krajalnik-Brown R, Parameswaran P, Marcus AK, Wanger G, Gorby YA, et al. Selecting anode-respiring bacteria based on anode potential: phylogenetic, electrochemical, and microscopic characterization. *Environ Sci Technol*. 2009;43:9519–24.
- Yang GQ, Huang LY, Yu Z, Liu XM, Chen SS, Zeng JX, et al. Anode potentials regulate *Geobacter* biofilms: new insights from the composition and spatial structure of extracellular polymeric substances. *Water Res*. 2019;159:294–301.
- Ying XB, Guo K, Chen W, Gu Y, Shen DS, Zhou YY, et al. The impact of electron donors and anode potentials on the anode-respiring bacteria community. *Appl Microbiol Biot*. 2017;101:7997–8005.
- Abdi H, Williams LJ. Principal component analysis. *Wires Comput Stat*. 2010;2:433–59.
- Ringner M. What is principal component analysis? *Nat Biotechnol*. 2008;26:303–4.
- Wold S, Esbensen K, Geladi P. Principal component analysis. *Chemometr Intell Lab*. 1987;2:37–52.
- Brown MB, Forsythe AB. Robust tests for the equality of variances. *J Am Stat Assoc*. 1974;69:364–7.
- Schloss PD, Westcott SL. Assessing and improving methods used in operational taxonomic unit-based approaches for 16S rRNA gene sequence analysis. *Appl Environ Microb*. 2011;77:3219–26.
- Shannon CE. A mathematical theory of communication. *Bell Syst Tech J*. 1948;27:379–423.
- Smith B, Wilson JB. A consumer's guide to evenness indices. *Oikos*. 1996;76:70–82.
- Gower JC. Principal coordinates analysis. In: Balakrishnan N, Colton T, Everitt B, Piegorsch W, Ruggeri F, Teugels JL, editors. *Wiley StatsRef: Statistics Reference Online*; 2015.
- Beals EW. Bray-Curtis ordination: an effective strategy for analysis of multivariate ecological data. *Adv Ecol Res*. 1984;14:1–55.
- Pearson K. On lines and planes of closest fit to systems of points in space. *Philos Mag*. 1901;2:559–72.
- Olsen RL, Chappell RW, Loftis JC. Water quality sample collection, data treatment and results presentation for principal components analysis – literature review and Illinois River watershed case study. *Water Res*. 2012;46:3110–22.
- Fricke K, Harnisch F, Schroder U. On the use of cyclic voltammetry for the study of anodic electron transfer in microbial fuel cells. *Energy Environ Sci*. 2008;1:144–7.
- Busalmen JP, Esteve-Nunez A, Feliu JM. Whole cell electrochemistry of electricity-producing microorganisms evidence an adaptation for optimal exocellular electron transport. *Environ Sci Technol*. 2008;42:2445–50.
- Parot S, Delia ML, Bergel A. Forming electrochemically active biofilms from garden compost under chronoamperometry. *Bioresour Technol*. 2008;99:4809–16.
- Hari AR, Katuri KP, Gorron E, Logan BE, Saikaly PE. Multiple paths of electron flow to current in microbial electrolysis cells fed with low and high concentrations of propionate. *Appl Microbiol Biot*. 2016;100:5999–6011.
- Schroder U. Anodic electron transfer mechanisms in microbial fuel cells and their energy efficiency. *Phys Chem Chem Phys*. 2007;9:2619–29.
- Bond DR, Lovley DR. Electricity production by *Geobacter sulfurreducens* attached to electrodes. *Appl Environ Microb*. 2003;69:1548–55.
- Geelhoed JS, Stams AJM. Electricity-assisted biological hydrogen production from acetate by *Geobacter sulfurreducens*. *Environ Sci Technol*. 2011;45:815–20.
- Speers AM, Reguera G. Electron donors supporting growth and electroactivity of *Geobacter sulfurreducens* anode biofilms. *Appl Environ Microb*. 2012;78:437–44.
- Zhu XP, Yates MD, Logan BE. Set potential regulation reveals additional oxidation peaks of *Geobacter sulfurreducens* anodic biofilms. *Electrochem Commun*. 2012;22:116–9.
- Marsili E, Sun J, Bond DR. Voltammetry and growth physiology of *Geobacter sulfurreducens* biofilms as a function of growth stage and imposed electrode potential. *Electroanal*. 2010;22:865–74.
- Baek G, Kim J, Lee S, Lee C. Development of biocathode during repeated cycles of bioelectrochemical conversion of carbon dioxide to methane. *Bioresour Technol*. 2017;241:1201–7.
- Zhang GD, Zhao QL, Jiao Y, Zhang JN, Jiang JQ, Ren N, et al. Improved performance of microbial fuel cell using combination biocathode of graphite fiber brush and graphite granules. *J Power Sources*. 2011;196:6036–41.
- Rabaey K, Read ST, Clauwaert P, Freguia S, Bond PL, Blackall LL, et al. Cathodic oxygen reduction catalyzed by bacteria in microbial fuel cells. *ISME J*. 2008;2:519–27.
- Wu YN, Zhao X, Jin M, Li Y, Li S, Kong FY, et al. Copper removal and microbial community analysis in single-chamber microbial fuel cell. *Bioresour Technol*. 2018;253:372–7.
- Chakraborty I, Bhowmick GD, Nath D, Khuman CN, Dubey BK, Ghangrekar MM. Removal of sodium dodecyl sulphate from wastewater and its effect on anodic biofilm and performance of microbial fuel cell. *Int Biodeter Biodegr*. 2021;156:105108.
- Freguia S, Tsujimura S, Kano K. Electron transfer pathways in microbial oxygen biocathodes. *Electrochim Acta*. 2010;55:813–8.
- Kumar A, Hsu LHH, Kavanagh P, Barriere F, Lens PNL, Lapinonniere L, et al. The ins and outs of microorganism-electrode electron transfer reactions. *Nat Rev Chem*. 2017;1:0024.
- Fedorovich V, Knighton MC, Pagaling E, Ward FB, Free A, Goryanin I. Novel electrochemically active bacterium phylogenetically related to *Arcobacter butzleri*, isolated from a microbial fuel cell. *Appl Environ Microb*. 2009;75:7326–34.
- Hassan H, Jin B, Donner E, Vasileiadis S, Saint C, Dai S. Microbial community and bioelectrochemical activities in MFC for degrading phenol and producing electricity: microbial consortia could make differences. *Chem Eng J*. 2018;332:647–57.
- Lam BR, Barr CR, Rowe AR, Nealon KH. Differences in applied redox potential on cathodes enrich for diverse electrochemically active microbial isolates from a marine sediment. *Front Microbiol*. 2019;10:01979.

## Publisher's Note

Springer Nature remains neutral with regard to jurisdictional claims in published maps and institutional affiliations.